

COMPARISON of INPUT PARAMETERS
USED for PHOTON TRANSPORT in the
UCI AND QUEENS MONTE CARLO'S and the
OUTPUT of THEIR ALGORITHMS

W. Frati M. Lowry and P. Skensved

May 23, 1991

I. INTRODUCTION

The Queens MC has been transported to Princeton's SPARC work station and the UCI code to the IBM R/6000 workstations at Penn and Guelph. Comparison of results from Queens, Princeton and Penn showed discrepancies of up to 30% in the number of PMT's required for a given percentage coverage. To investigate the source of these discrepancies several parameters were compared: a) reflector shape; b) Cerenkov photon scattering and absorption in Acrylic, D₂O , and H₂O ; c) PMT response as a function of wavelength.

II REFLECTOR SHAPE

Princeton, running the Queens code, and Penn, running the UCI code, found significantly less coverage ($\approx 30\%$) with 9500 PMT's than Queens, running the Queens code. The major contributor to this difference was in the size of the reflectors used. Penn and Princeton used the "standard" 190 mm Oxford cone (reproduced in Fig 1), which covers 190 mm of the PMT surface and subtends an angle of 49° with the PMT's center of curvature, while Queens used its own design which covers 210 mm and 59.3°. The parameters used to define the cones are given in Appendix I. Note that while Princeton and Penn use different parametrizations, the shapes comes out to be virtually identical and agree well with the numerical table issued by Oxford.

III ACRYLIC ATTENUATION

Fig 2 shows the input attenuation coefficient data, given in units of the inverse mean free path (IMFP), used by the Queens MC at Queens overlaid with that initially used by Princeton when running the Queens code. Queens takes the Polycast immersed in D₂O data from Tables 3 and 4 in SNO-STR-88-65 (Reproduced in Table I), while Princeton used the Redbook values for Polycast (Annex 2 to SNO-87-12, pg 4). The different inputs result in a 15% difference for the number of PMT's firing for a given

event. Table II summarizes the results from Queens and Princeton and demonstrates our sensitivity to uncertainties in the acrylic attenuation length. Princeton is currently using the data from SNO-STR-88-65.

The comparison of the data from SNO-STR-88-65 with the output generated by the Queens code is shown in Fig 3. (Arbitrary error bars are assigned to the data since none are quoted.) The comparison with the output generated by the UCI code is shown in Fig 4. Both codes reproduce the input data well, with the UCI code matching the data points a little better, but producing wiggles above 400 nm when interpolating between and beyond the data points

IV D2O SCATTERING and ATTENUATION

The input data for the attenuation coefficients are taken from L. P. Boivin et. al. Applied Optics Vol 25, No 6, 15 Mar 1986 and is reproduced in Table III. Attenuation and scattering were not measured separately resulting in an assumption made by both the Queens and UCI MC that the attenuation and scattering IMFP are equal at 400 nm. The UCI code incorrectly assumes they are equal at all wavelengths. The comparison of the output of the UCI code with the data is shown in Fig 5, where it is seen that the sum of the attenuation and scattering IMFP's from the UCI code matches the data fairly well. Above 600 nm the UCI extrapolation algorithm shows a rise which is probably incorrect.

The Queens code also starts with the assumption of equal scattering and attenuation IMFP's at 400 nm, but then assigns a $1/\lambda^4$ dependence to the inverse scattering length. The output of the Queens code for the attenuation, scattering and total IMFP is shown in Fig 6, with the sum of the scattering and attenuation IMFP agreeing well with the data.

A direct comparison of the data and output of the Queens and UCI MC's is shown in Fig 7.

V H2O SCATTERING and ATTENUATION

The input data is obtained from the above cited Applied Optics paper and is reproduced in Table III. Here again it is assumed that the scattering and attenuation coefficients are the same at 400 nm. Fig 8 compares the output of the Queens code

with the data, and there is good agreement between the two.

Here UCI uses the $1/\lambda^4$ dependence for the scattering coefficient, but its extrapolation of the attenuation coefficient below wavelengths of 400 nm causes the sum of the scattering and attenuation IMFP to be too large, as shown in Fig 9.

Fig 10 plots the UCI, Queens and Kamiokande calculations of the IMFP along with the data of Boivin et. al. for direct comparison.

VI - PMT PHOTOCATHODE RESPONSE

Fig 11 plots the relative quantum efficiency of the photocathode as a function of the wavelength for:

- 1) Hamamatsu specs (Smooth curve)
- 2) Output of the UCI algorithm
- 3) Input data used by the Queens MC. (Note that this is not the output generated by exercising the Queens code)

The UCI and Queens quantum efficiencies are identical, but will have to be upgraded to match the Hamamatsu specs. Note the extra bonus of the low radioactivity Schott glass in the improved response at the lower wavelengths.

APPENDIX I

Light Cone Parametrizations

$\theta_{cathode}$ = half angle subtended by photocathode

z = symmetry axis of PMT

ρ = radial distance from z axis

R = PMT photocathode radius

Lengths in mm

A) UCI Parametrization - Oxford Cone

The cone is defined using a variable θ as a parameter. $z = 0$ is at the center of the PMT photocathode radius and intercepts the PMT at $\rho = 95$ $z = 82.6$.

$$R = 126$$

$$\theta_{cathode} = 49^\circ$$

$$z = -R \times \cos(\theta) - t \times \sin(\theta)$$

$$\rho = R \times \sin(\theta) - t \times \cos(\theta)$$

$$t = R \times (\theta + \theta_{cathode} - \pi)$$

B) Princeton Parametrization - Oxford Cone

$z = 79.2$ is where the cone meets the PMT, for which $\rho = 95$.

$$R = 126$$

$$\left[\frac{\rho - 77.6}{51.3} \right]^2 + \left[\frac{(z - 79.2) - 147.0}{156.8} \right]^2 = 1$$

This is virtually identical to the UCI cone except the bottom $(82.6 - 79.2) = 3.4$ mm is lopped off compared to the the UCI parametrization.

C) Queens Cone

$z = 0$ is at the center of the PMT photocathode radius and intercepts the PMT at $\rho = 105.0$, $z = 62.2$, $\theta_{cathode} = 59.3^\circ$

$$R = 122$$

$$\left[\frac{\rho}{148.9} \right]^2 + \left[\frac{z - 237.7}{247.5} \right]^2 = 1$$

TABLE I

Attenuation Coefficient in Acrylic
Polycast in Deuterium

λ nm	Inverse Attenuation Length cm^{-1}
300	0.488
305	0.231
310	0.154
315	0.125
320	0.111
325	0.099
330	0.086
340	0.062
350	0.043
360	0.033
370	0.023
380	0.018
390	0.015
400	0.013
450	0.009
500	0.006

TABLE II

Average (RMS) Values of Queens MC Output

10 MeV Electrons

Generated at $(x,y,z) = (500,0,0)$ cmDirection Cosines $(\alpha, \beta, \gamma) = (0,0,1)$

	# Cerenkov Photons	# Photoelectrons	# Hit PMT
Queens SNO-STR-88-65	331.4(32.6)	121.7(14.4)	115.6(13.1)
Princeton Redbook	332.0(31.4)	107.6(13.7)	102.6(13.7)
Princeton SNO-STR-88-65	332.0(32.8)	124.0(14.8)	117.6(13.6)

TABLE IIIAttenuation Coefficient in D₂O and H₂O

λ nm	Inverse Attenuation Length 10^{-4}cm^{-1}	
	H ₂ O	D ₂ O
578	9.2(0.7)	1.1(0.7)
546	5.8(0.7)	1.2(0.7)
436	1.3(0.7)	2.4(0.7)
406	1.1 (0.7)	2.8(0.7)
366	1.4(0.7)	3.7(0.7)
313	4.1(0.7)	8.9(0.7)
254	15.2(4.2)	32.3(4.7)

Figure Captions

Fig 1. Standard 190 mm Oxford Cone

Fig 2. Acrylic attenuation length vs wavelength from a) SNO-STR-88-65 Arbitrary error bars are assigned to the these data; b) Red Book Annex 2 to SNO-87-12.

Fig 3. Acrylic attenuation length vs wavelength from SNO-STR-88-65 overlaid with the output of the Queens MC algorithm.

Fig 4. Acrylic attenuation length vs wavelength from SNO-STR-88-65 overlaid with the output of the UCI MC algorithm.

Fig 5. Overlays of the total inverse mean free path of D_2O from Data, Queens MC, and UCI MC.

Fig 6. Attenuation, scattering and total inverse mean free path for D_2O from the Queens MC, overlaid with the measured total.

Fig 7. Attenuation, scattering and total inverse mean free path for D_2O from the UCI MC, overlaid with the measured total.

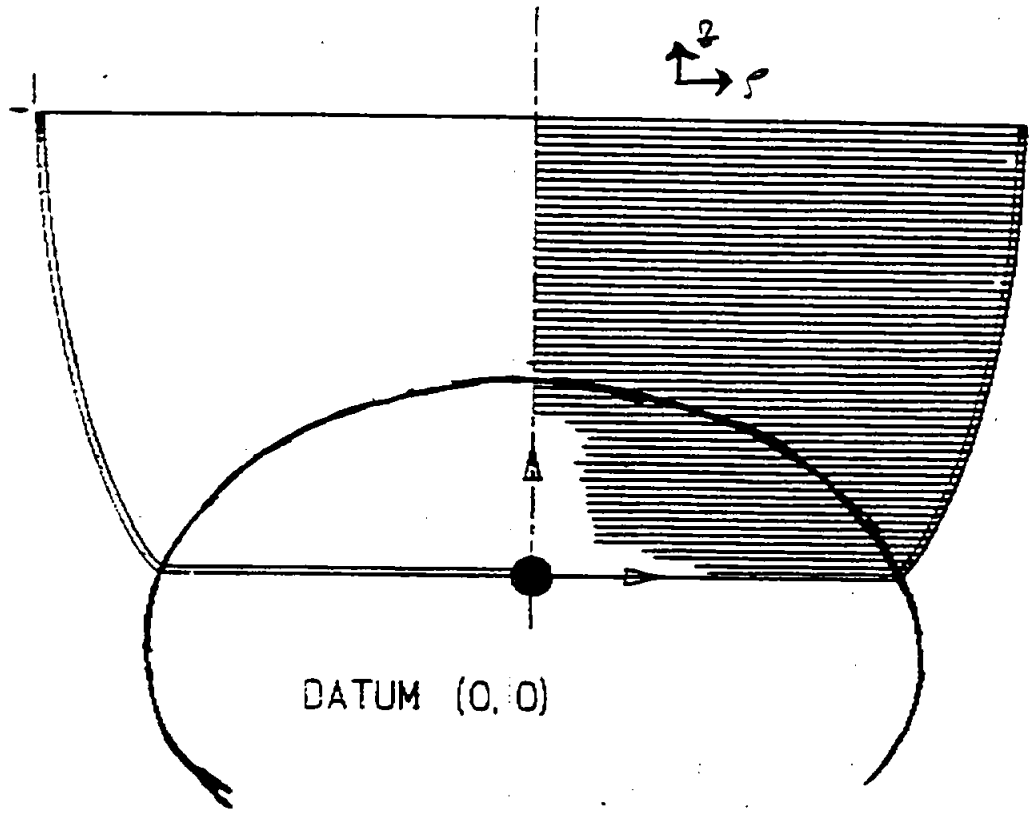
Fig 8. Attenuation, scattering and total inverse mean free path for H_2O from the Queens MC, overlaid with the measured total.

Fig 9. Attenuation, scattering and total inverse mean free path for H_2O from the UCI MC, overlaid with the measured total.

Fig 10. Total inverse mean free path in H_2O from Data, Queens MC, UCI MC, and Kamiokande.

Fig 11. Photocathode response vs wavelength for the 8" Hamamatsu PMT. Solid line is from the specifications sheet.

r	s
3.00	94.9
5.23	96.47
9.36	98.18
5.06	99.68
6.92	100.90
9.06	102.14
11.01	103.22
12.98	104.27
14.99	105.27
17.00	106.24
19.03	107.17
21.08	108.08
23.14	108.95
25.22	109.8
27.32	110.62
29.42	111.42
31.54	112.2
33.68	112.95
35.82	113.67
37.98	114.38
40.14	115.06
42.32	115.72
44.5	116.36
46.70	116.98
48.90	117.58
51.11	118.17
53.33	118.73
55.56	119.27
57.79	119.80
60.03	120.30
62.28	120.79
64.53	121.26
66.78	121.72
69.04	122.16
71.31	122.58
73.58	122.98
75.86	123.37
78.14	123.74
80.42	124.10
82.71	124.44
85.00	124.77
87.29	125.08
89.58	125.38
91.88	125.66
94.18	125.93
96.48	126.19
98.79	126.43
101.1	126.66
103.41	126.87
105.72	127.07
108.03	127.26
110.32	127.44
112.66	127.60
114.98	127.75
117.29	127.89
119.61	128.02



TOLERANCES UNLESS STATED	UNIVERSITY OF OXFORD. P1	
	MATERIAL	SURFACE FINISHNESS U.O.A. UNLESS STATED FINISH
ORIGINAL SCALE 1/1	TITLE	

Fig. 1

Acrylic Attenuation

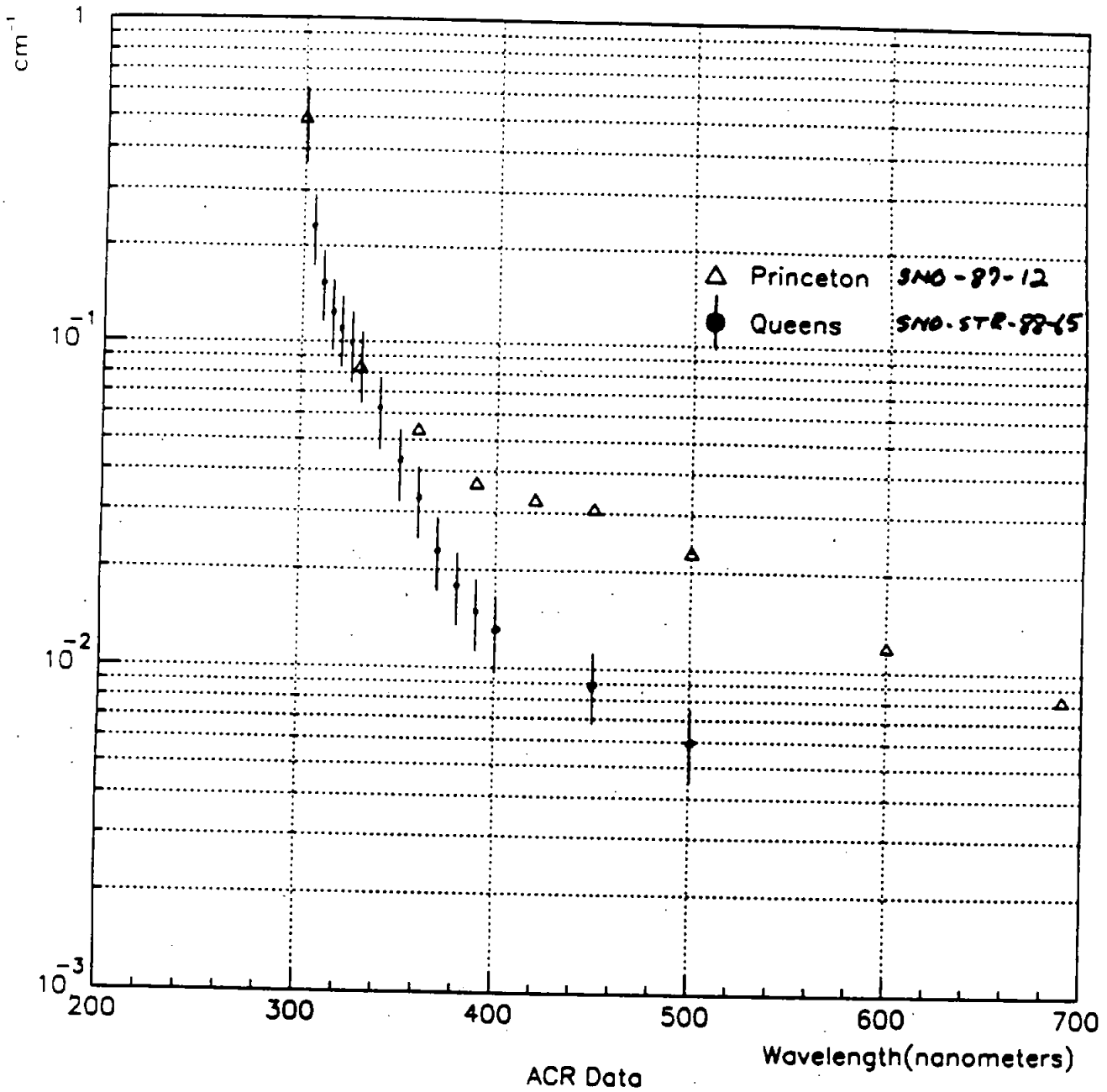
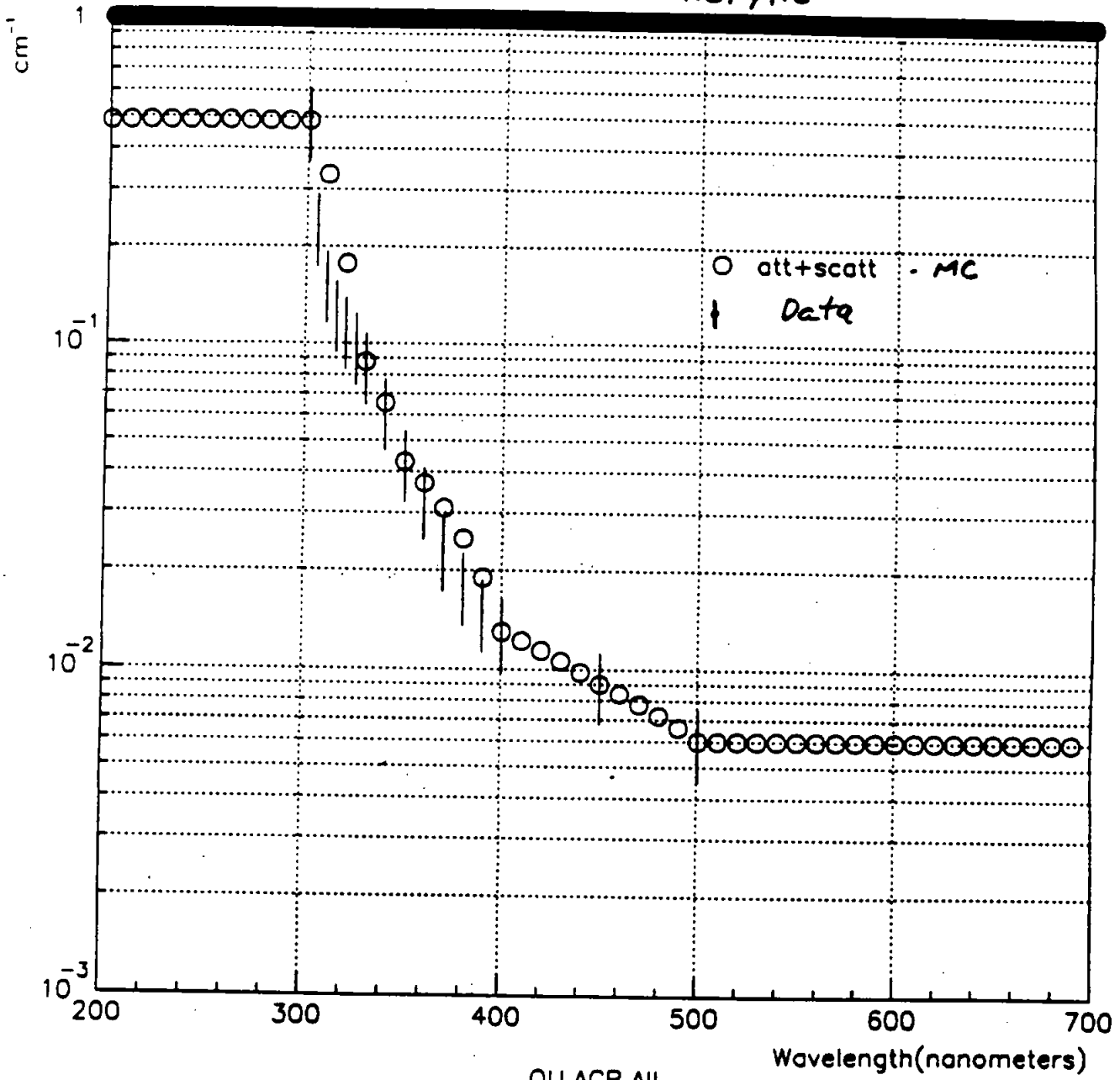


Fig. 2

Acrylic



QU ACR AII

Fig. 3

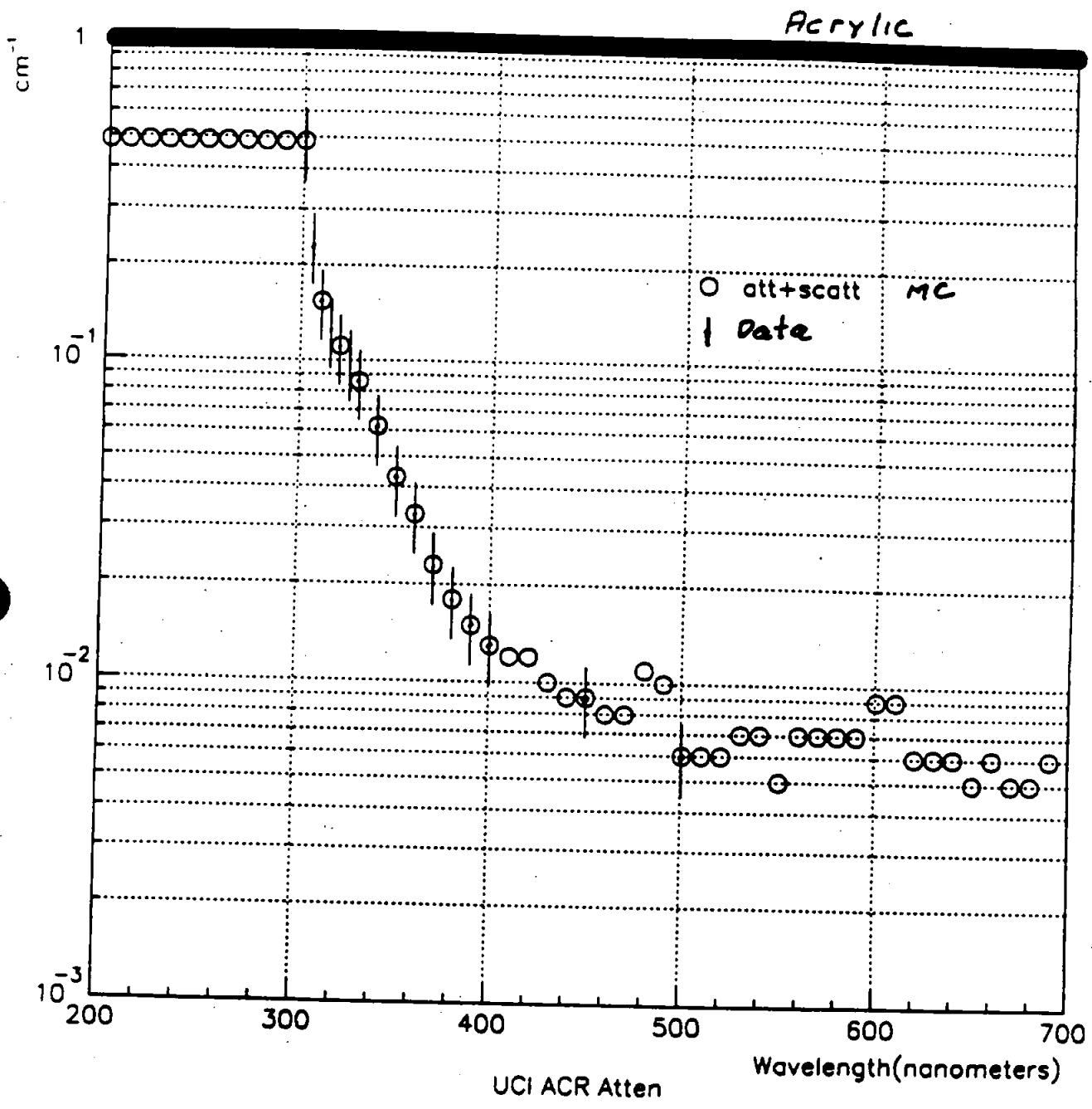


Fig. 4

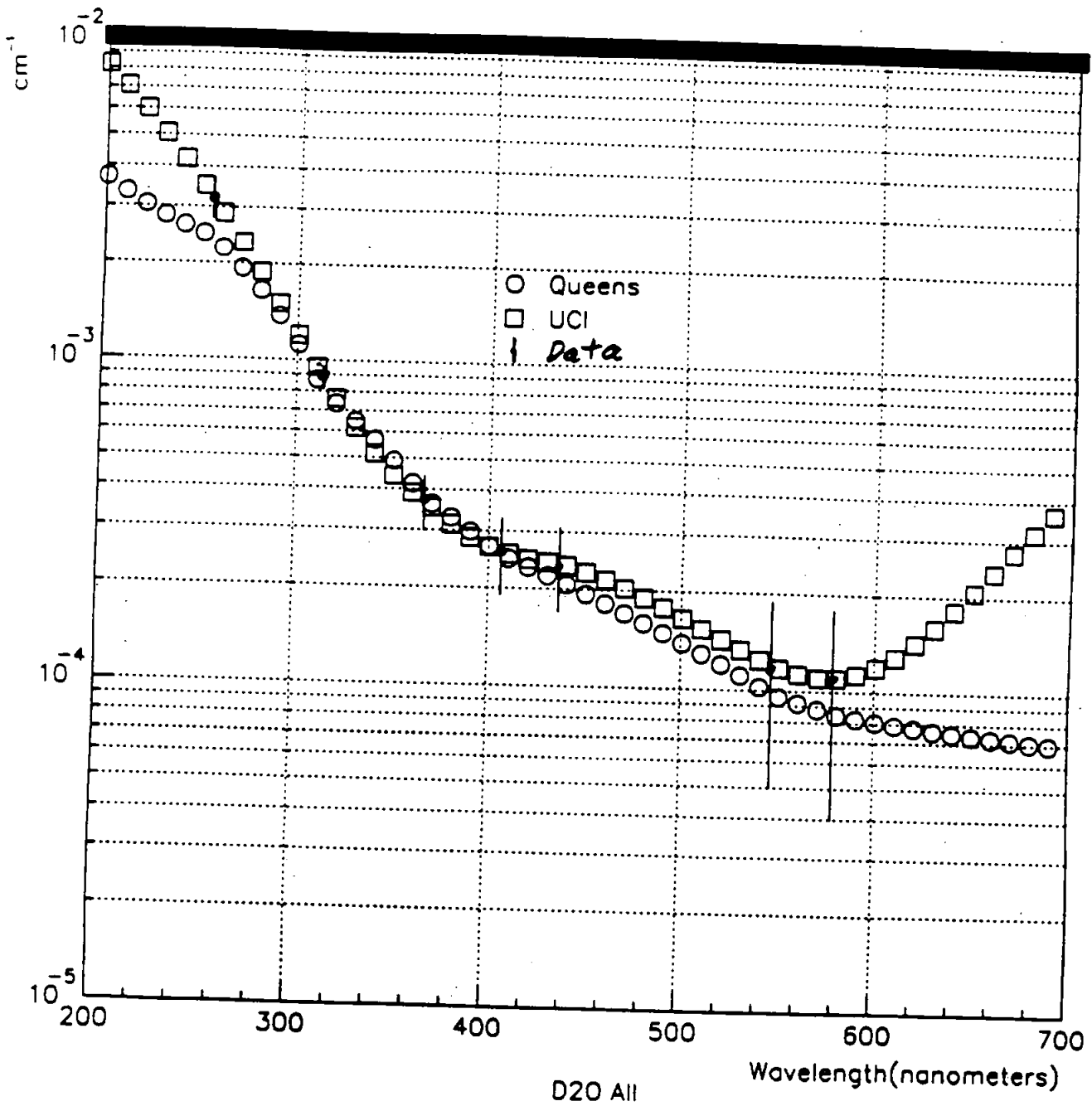


Fig. 5

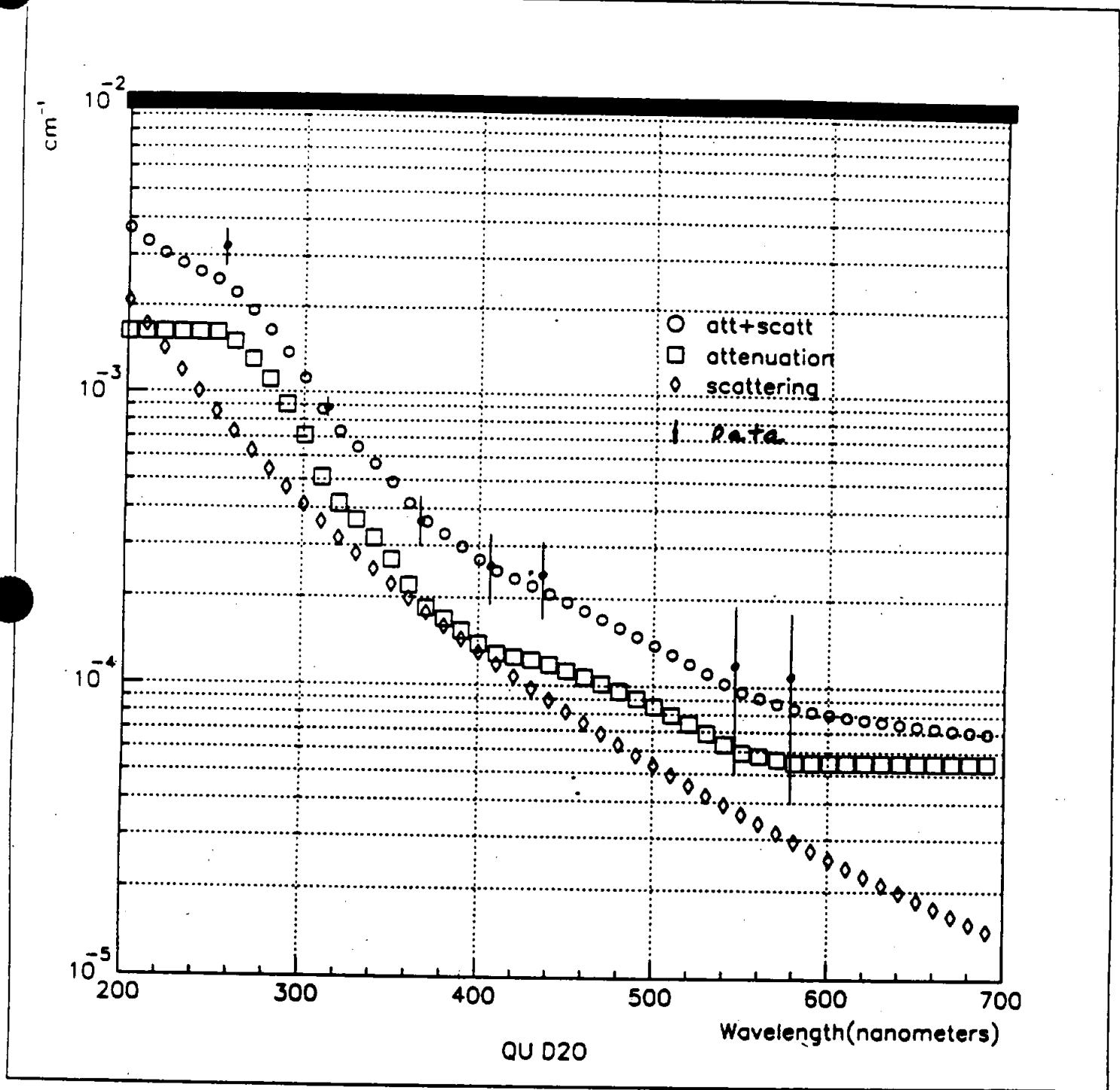
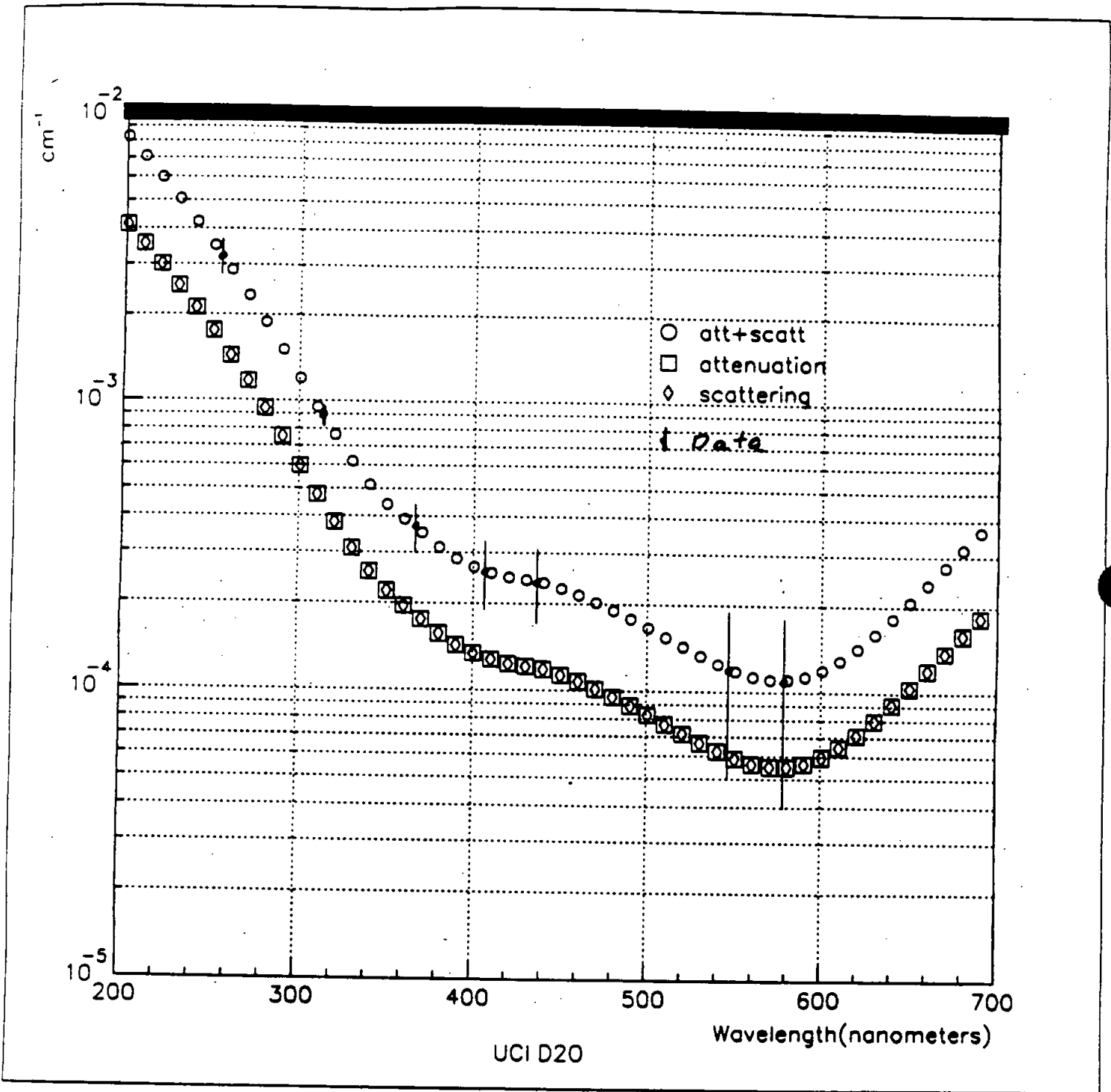


Fig. 6



UCI D20

Fig. 7

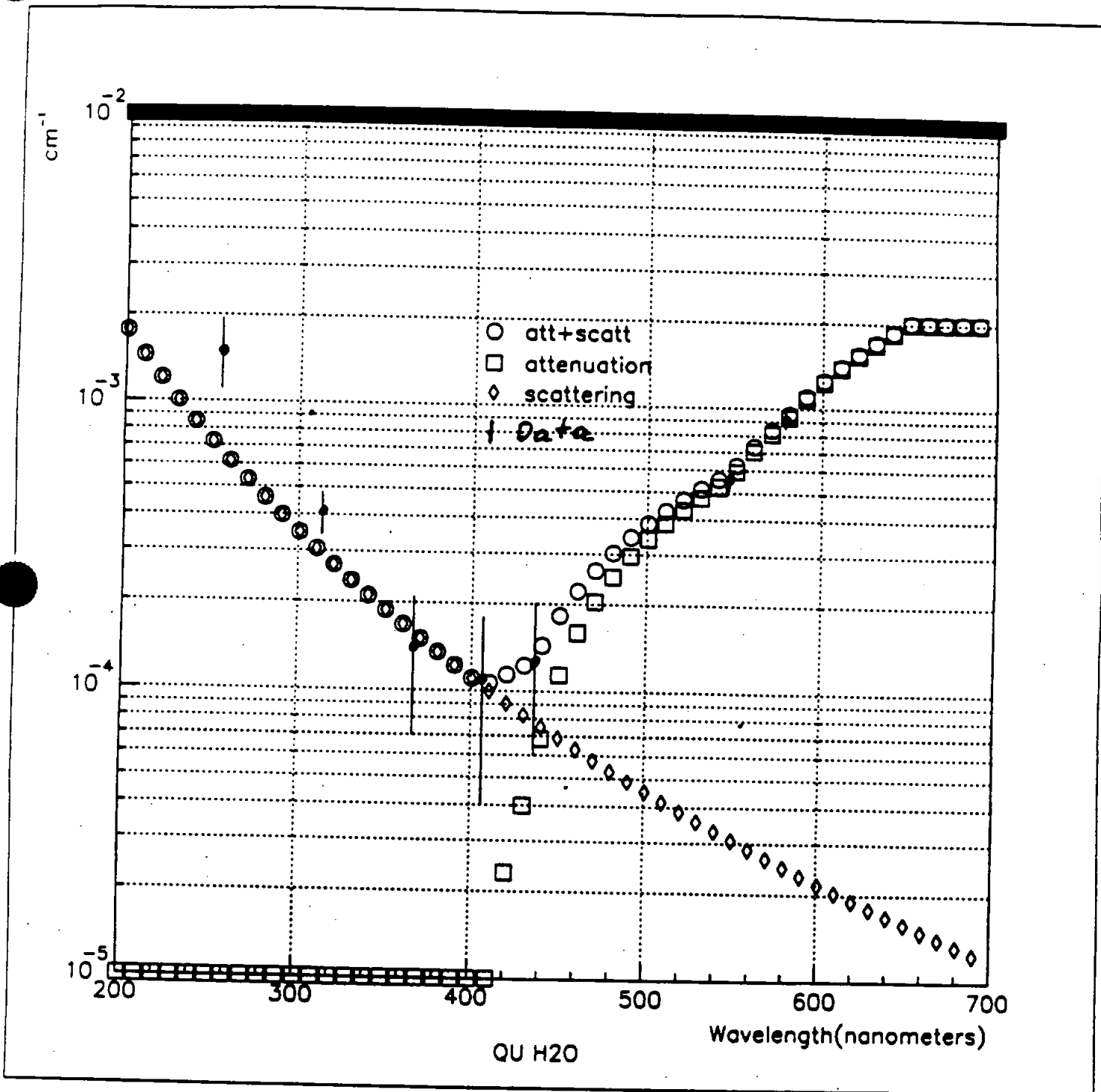


Fig. 8

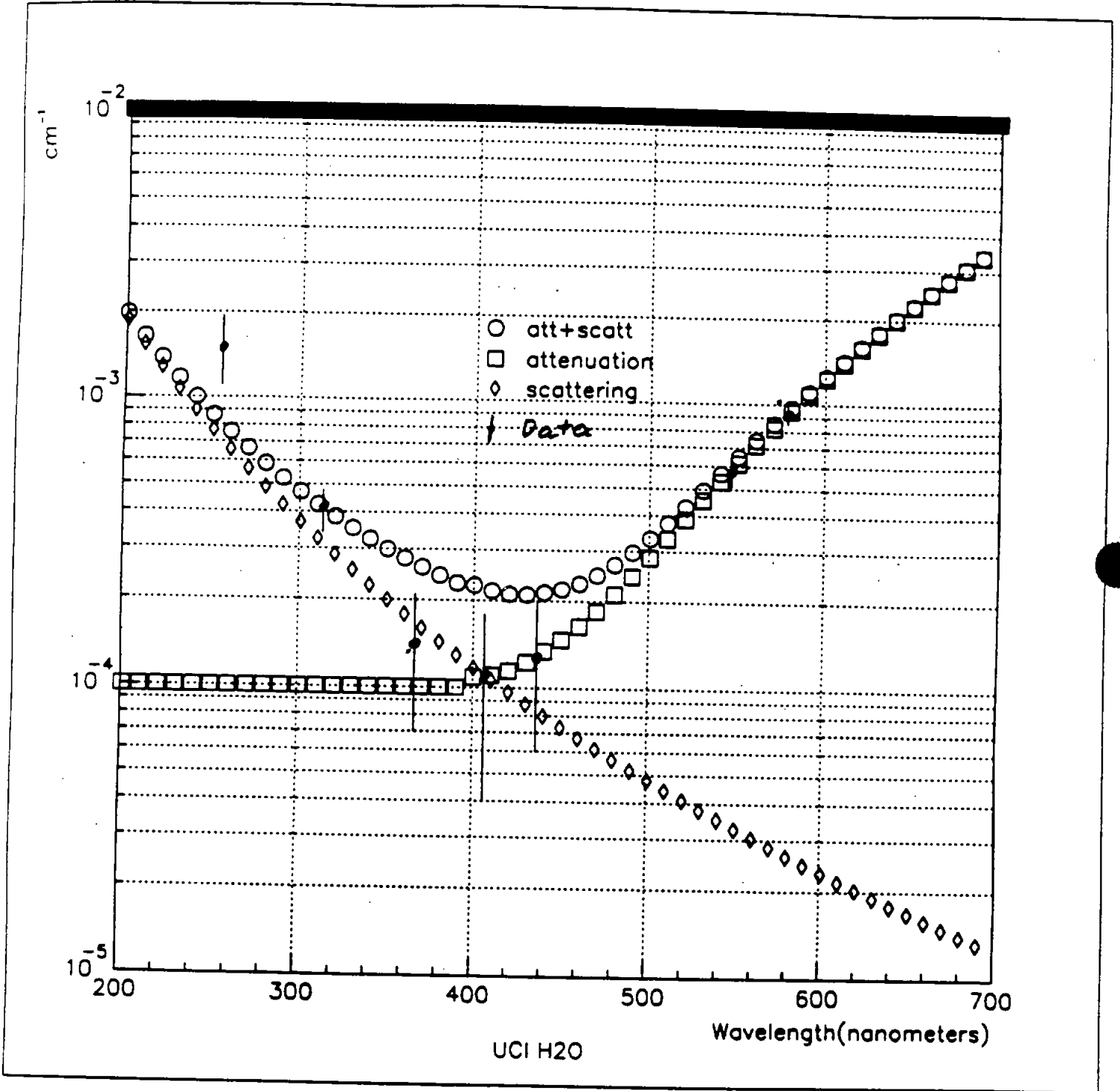


Fig. 9

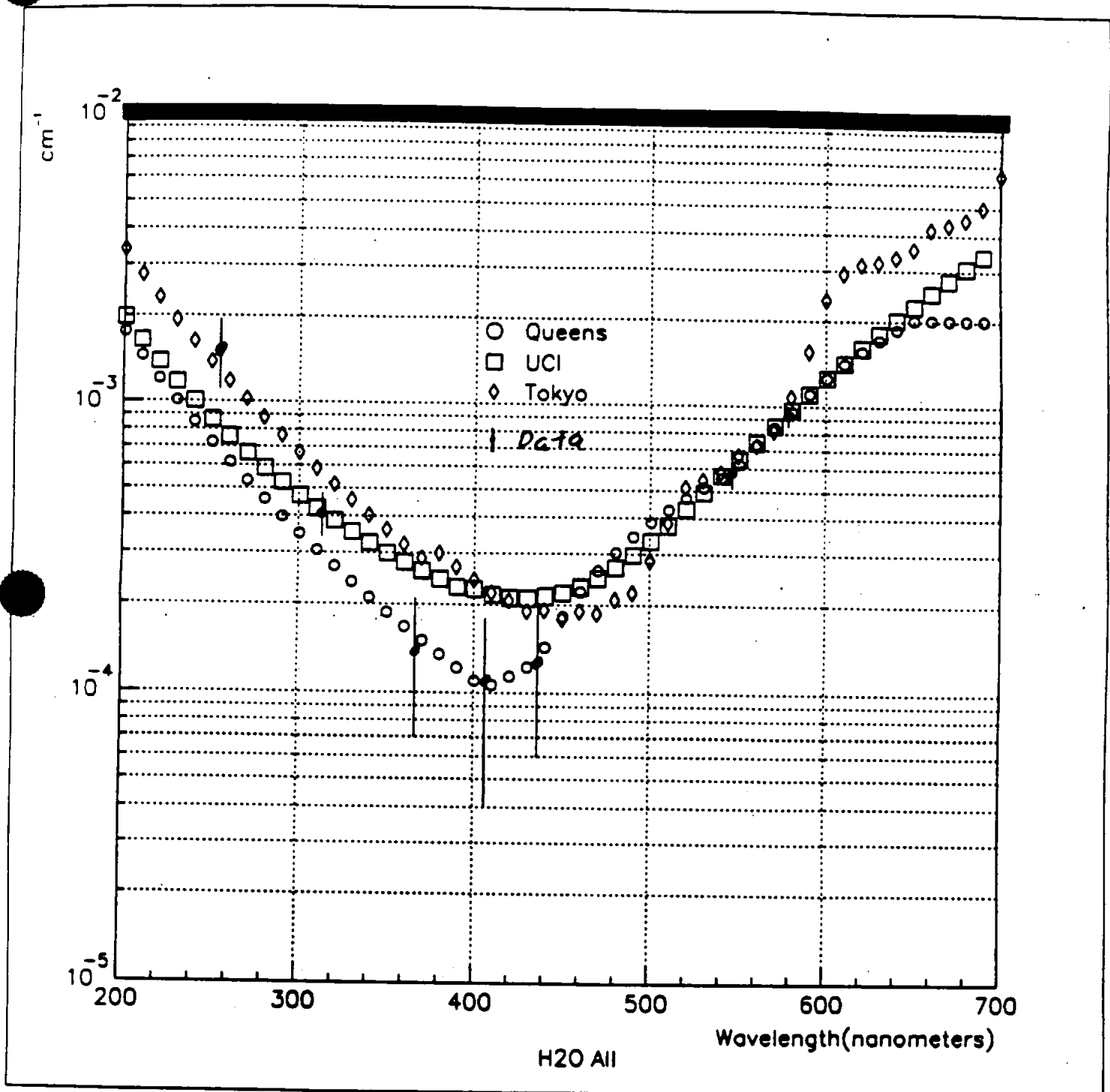


Fig. 10

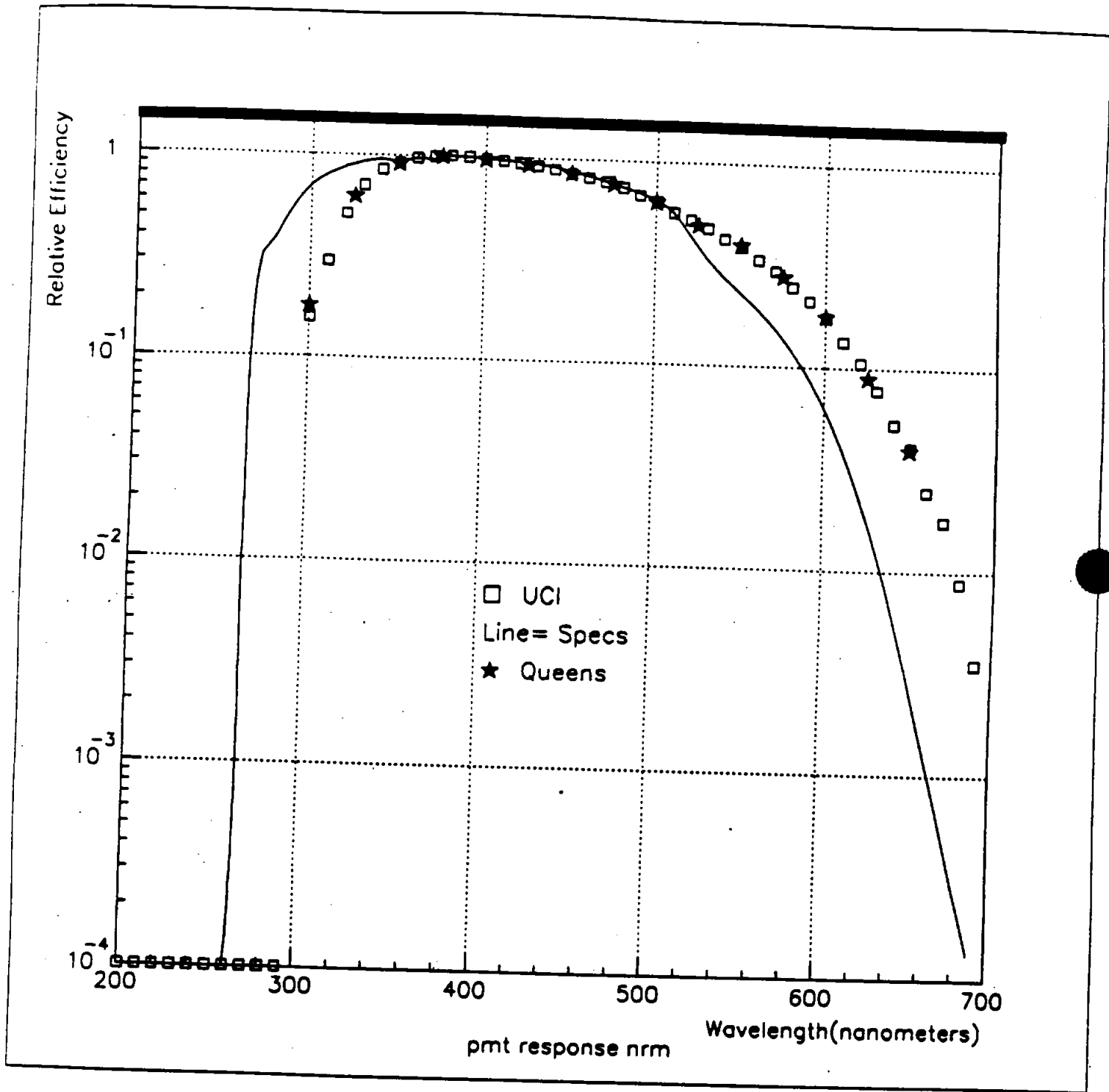


Fig 11